

1 **Design of chondroitin sulfate-based polyelectrolyte nanoplexes:**
2 **formation of nanocarriers with chitosan and a case study of salmon**
3 **calcitonin**
4

Anita Umerska^{a,b}, Owen I. Corrigan^a, Lidia Tajber^{a*}

*To whom correspondence should be addressed: lidia.tajber@tcd.ie

Phone: 00353 1 896 2787 Fax: 00353 1 896 2810

Affiliation:

a) School of Pharmacy and Pharmaceutical Sciences, Trinity College Dublin, Dublin 2, Ireland.

b) INSERM U1066, Micro et Nanomédecines Biomimétiques, Angers, France.

Email addresses of authors:

Anita Umerska – umerskam@tcd.ie

Owen I. Corrigan – corrign@tcd.ie

Lidia Tajber – lidia.tajber@tcd.ie

5

6 **Abstract**

7 The aim of this work was to examine the formation and properties of chondroitin sulfate
8 (CHON)-based nanoparticles (NPs), namely CHON/chitosan (CHIT), CHON/CHIT/calcitonin
9 (sCT) and CHON/sCT. Both, positively and negatively charged CHON/CHIT NPs have been
10 successfully obtained with properties that were dependent on the polymer mixing ratio,
11 polymer concentration and molecular weight of CHIT. sCT was successfully loaded into
12 CHON/CHIT NPs with efficiency close to 100% and notably high loading (up to 33%). A new
13 type of NPs composed of CHON and sCT (a binary system) has been successfully
14 developed. CHON/sCT NPs offer the advantage of a very high drug loading up to 73%. The
15 particle size of CHON-based NPs increased in PBS, acetate buffer and in HCl solution
16 compared to that in water, but most of them remained in the nano-range even after 24 hours.
17 The media and composition of the nanocarriers were found to affect the release of sCT.

18

19 **Keywords**

20 Chondroitin sulfate ; chitosan ; nanoparticles ; polyelectrolyte complexes ; calcitonin ;
21 peptide

22 1. Introduction

23 Traditionally, pharmaceutical excipients are treated as “inert” materials and are not
24 expected to have pharmacological activity (Baldrick, 2010), however this view has changed
25 as newly approved excipients cover a range of functions from stabilizing formulations to
26 active roles of enhanced drug uptake and specific drug delivery (Goole et al., 2010).
27 Pharmaceutical polymers bearing a charge, polyelectrolytes, have been extensively studied
28 as components of micro- and nano-sized carriers for the delivery of a range of therapeutic
29 molecules such as peptides and nucleic acids. Among polyelectrolytes, cationic and anionic
30 polysaccharides have received particular attention and some of them also have interesting
31 pharmacological properties. For instance hyaluronic acid (HA) has been shown to act in
32 synergy with salmon calcitonin (sCT) reducing inflammatory biomarkers *in vitro* and
33 inflammatory arthritis *in vivo* (Ryan et al., 2013). Another glycosaminoglycan, chondroitin
34 sulfate (CHON) has been used for the preparation of nanocarriers for drug/gene delivery
35 (Zhao, Liu, Wang & Zhai, 2015). CHON is an unbranched polysaccharide containing two
36 alternating monosaccharides: D-glucuronic acid and N-acetyl-D-galactosamine. It is an
37 abundant glycosaminoglycan found in cartilage, bone and connective mammalian tissue.
38 CHON is a symptomatic slow-acting agent for osteoarthritis, commonly sold together with
39 glucosamine. It has been shown to be absorbed after oral administration in humans as a
40 high molecular weight polysaccharide (Volpi, 2002), therefore it has a potential to be used to
41 increase the absorption of encapsulated molecules. Coating of chitosan (CHIT) NPs with
42 CHON increased the uptake of the encapsulated nucleic acid by COS7 cells (transformed
43 African green monkey kidney fibroblasts) via interaction of CHON with CD44 receptors
44 (Hagiwara, Nakata, Koyama & Sato, 2012).

45 CHON has weak, carboxylate, and strong, sulfate, moieties attached to the main
46 glycan backbone. Due to its acidic nature CHON is able to produce ionic complexes with
47 cationic molecules (Denuziere, Ferrier & Domard, 1996). Examples of such complexes
48 include CHON complexes with protamine (PROT) (Umerska et al., 2015), lysozyme (van
49 Damme, Moss, Murphy & Preston 1994), trimethylchitosan (Place, Sekyi & Kipper, 2014),

50 however most of the polyelectrolyte complexes of CHON tested thus far are those with CHIT
51 (Yeh, Cheng, Hu, Huang & Young, 2011; Tsai et al., 2011; Santo, Gomes, Mano & Reis,
52 2012; Place et al., 2014). CHIT is a linear polysaccharide composed of randomly distributed
53 D-glucosamine (deacetylated unit) and N-acetyl-D-glucosamine (acetylated unit) linked via
54 β -(1 \rightarrow 4)-glycosidic bonds. The properties of CHIT can be useful in medicine, as it reduces
55 bleeding (Pusateri et al., 2003) and has antibacterial activity (Benhabiles et al., 2012). Due
56 to its mucoadhesive properties it could be a valuable component of drug delivery systems
57 (Sogias, Williams & Khutoryanskiy, 2008).

58 Further research on NPs containing CHON and CHIT is required, as to the best of
59 our knowledge no systematic investigation on the formation of both, positively and negatively
60 charged CHON/CHIT NPs, has been published to date. The charge is of a key importance in
61 cellular uptake and cytotoxicity of medical NPs (Fröhlich, 2012). For instance it has been
62 shown that positively charged HA/CHIT NPs exerted toxic effects on Caco-2 cells in contrast
63 to negatively charged NPs (Umerska et al., 2012). Initially the studies on CHON nanocarriers
64 focused on the employment of CHON as an agent to yield positively charged CHIT NPs
65 intended for the encapsulation of molecules like FITC-BSA (Yeh et al., 2011), BSA (Santo et
66 al., 2012), doxorubicin (Hu et al., 2014), Nell-1 protein (Hou, Hu, Park & Lee, 2012). The
67 NPs obtained in those studies were characterized by a positive charge. Recently,
68 CHON/CHIT NPs containing CHON as the main ingredient were produced as aggrecan
69 mimicking NPs (Place et al., 2014). However, none of these studies considered the
70 stoichiometry of CHON/CHIT NPs formation. Hence the aim of this paper was to examine
71 the stoichiometry of molecular interactions between CHON and CHIT within CHON/CHIT
72 NPs. Another objective was to discuss the criteria of carrier selection and to select carriers
73 with optimal properties for the encapsulation of a cationic peptide, sCT. Knowing the
74 principles and approach to loading this peptide, the same criteria could be translated to
75 encapsulating similar cationic therapeutically relevant molecules, such as antimicrobial
76 peptides and growth factors.

77 Similarly to HA, CHON NPs are interesting as carriers for sCT due to complementary
78 pharmacological action of both molecules (Umerska et al., 2015). As in some instances the
79 presence of CHIT may not be necessary, and there is evidence that CHON forms complexes
80 with sCT (Umerska et al., 2015), the purpose of this paper was to design and characterize
81 CHON/sCT NPs. Cationic molecules, e.g. CHIT, could compete with sCT for binding with
82 CHON molecules. Because the colloidal stability of polyelectrolyte complex NPs depends on
83 their charge, the incorporation of large quantity of sCT could lead to destabilization of the
84 system. Eliminating cationic CHIT from the formulation could offer the advantage of a very
85 high sCT loading. The last objective of this paper was to examine the influence of the
86 composition of the nanocarrier on the stability in different environments and the peptide
87 release.

88 **2. Materials and methods**

89 **2.1 Materials**

90 Chondroitin 4-sulfate sodium salt (CHON) was purchased from Sigma (Ireland).
91 Salmon calcitonin (sCT, as acetate salt) was obtained from PolyPeptide Laboratories.
92 Chitosan chlorides were obtained from Chitoceuticals (Germany) (referred to as CL42) and
93 Novamatrix (Norway) (Protasan UP CL113, referred to as CL113). All other reagents,
94 chemicals and solvents were of analytical grade.

95 **2.2 Physicochemical characterization of polymers**

96 The molecular weight of polymers was determined using a gel permeation
97 chromatography system previously described (Umerska et al., 2012). For CHIT samples, the
98 mobile phase was composed of 0.33 M acetic acid and 0.2 M sodium acetate. For a CHON
99 sample, the mobile phase was composed of 0.2M NaCl and 0.01M NaH₂PO₄ brought to pH
100 7.4 with NaOH solution. Determination of the chloride ions was performed with a Dr Lange
101 LCK 311 test as described earlier (Parojčić et al., 2011). The content of sodium counterion
102 was determined by inductively coupled plasma-mass spectrometry (ICP-MS) (Paluch et al.,
103 2010). NMR experiments on the degree of deacetylation of CHIT was done as described
104 previously (Umerska et al., 2012).

105 **2.3 Preparation of CHON/CHIT, CHON/CHIT/sCT and CHON/sCT nanoparticles**

106 The CHON solutions, CL42 solutions, CL113 solutions and sCT solutions were
107 prepared in deionized water. A predefined aliquot of the sCT solution and/or the CHIT
108 solution was added to a known volume of the CHON solution (one shot addition) at room
109 temperature under stirring; the stirring was maintained to allow for stabilization of the
110 system. A dispersion of particles was instantaneously obtained upon mixing of polymer
111 solutions.

112 Charge mixing ratio (CMR) was calculated by dividing the total number of negatively
113 charged ionizable groups (n^-) by the total number of positively charged ionizable groups (n^+)
114 considering the counterion content, the deacetylation degree of CHIT and pH.

115 **2.4 Nanoparticle characterization**

116 Transmittance and pH of the NP dispersions were measured as described by
117 Umerska et al. (2012). Dynamic viscosity measurements were carried out using an SV-10
118 Vibro Viscometer (A&D Company Limited). The amount of free or NP-associated polymer
119 (CHON for negatively charged NPs; CHIT for positively charged NPs) was determined from
120 viscosity measurements of continuous phases of NP dispersions. The viscosity of pure
121 polymer solution, for a given polymer concentration, was taken as containing 100% free
122 polymer, whereas the viscosity of water was taken as containing 0% free polymer. The
123 percentage of NP-associated polymer was calculated as a difference between the starting
124 quantity of polymer used in formulation (using the initial polymer concentration) and the
125 quantity of free/non-associated polymer (Umerska et al., 2015). The calculations are based
126 on assumptions that the contribution of NPs, any possible soluble complex formed between
127 the polymers and electrolyte ions originating from the polymers to the viscosity of the
128 systems is negligible. This was corroborated by the fact that viscosity of the CHON/CHIT
129 systems with a mass mixing ratio of 1.25 containing stoichiometric quantities of both
130 polymers was 0.89 ± 0.01 mPa·s, which is not significantly different to that of pure water at 25
131 °C.

132 The intensity-averaged mean particle size (hydrodynamic particle diameter) and
133 polydispersity index were determined by dynamic light scattering (DLS) using 173°
134 backscatter detection. The electrophoretic mobility values measured by laser Doppler
135 velocimetry (LDV) were converted to zeta potential by the Smoluchowski equation. Both DLS
136 and LDV measurements were done as described by Umerska et al., (2012). The obtained
137 results were corrected for the sample viscosity measured as described above.

138 **2.5 Salmon calcitonin (sCT) loading studies**

139 **2.5.1 Separation of non-associated sCT**

140 Non-associated sCT was separated from the NPs using a combined ultrafiltration-
141 centrifugation technique (Amicon® Ultra-15, MWCO of 30 kDa, Millipore, USA) as described
142 by Umerska et al., (2015). The filtrate containing non-associated sCT was assayed via high
143 performance liquid chromatography (HPLC), as described in Section 2.5.4. The association
144 efficiency (AE) and drug loading (DL) were calculated as described by Umerska, Corrigan &
145 Tajber (2014a).

146 **2.5.2 Colloidal behavior of CHON/CHIT/sCT and CHON/sCT NPs in different media**

147 Aliquots of 250 µl of the NPs were added to 2.25 ml of the dispersant. The following
148 dispersants were used: (1) phosphate-buffered saline (PBS) pH=7.4, (2) PBS pH=7.4 diluted
149 with deionized water (1:10), (3) acetate buffer pH=5, (4) acetate buffer pH=5 diluted with
150 deionized water (1:10), (5) deionized water and (6) HCl 0.07M pH=1.2 (Umerska et al.,
151 2015). Samples were incubated at 37 °C at 100 rpm. Size and zeta potential measurements
152 (Section 2.4) were performed after 1 hour and 24 hours of incubation.

153 **2.5.3 Release studies**

154 Aliquots of 250 µl of sCT-loaded NPs were added to 2.25 ml of dispersant and
155 incubated at 37 °C at 100 rpm (see Section 2.5.2). After 1, 2, 4, 6 and 24 hours, 2.5 ml
156 aliquots were withdrawn, and the released sCT was separated using the combined
157 ultrafiltration-centrifugation technique as described by Umerska et al. (2015). The data from
158 the release studies were fitted to the first-order equation:

159 $W = W_{\infty}(1 - e^{-kt})$ (Eqn. 1)

160 where W is the amount of the peptide released at time t (based on cumulative release), W_{∞}
 161 is the amount of the peptide released at infinity and k is the release rate constant.

162 **2.5.4 Quantification of sCT**

163 Analysis of sCT content was performed using an HPLC system as described
 164 previously (Umerska et al., 2014a). Briefly, 50 μ l of the standard or sample was injected into
 165 the Jones Chromatography Genesis 4 μ C18 150x4.6 mm column. A flow rate of 1 ml/min
 166 was employed using a mobile phase composed of 0.116% w/v NaCl, 0.032% v/v
 167 trifluoroacetic acid and 34% v/v acetonitrile. The UV detection was carried out at 215 nm.

168 **2.6 Statistical analysis**

169 The statistical significance of the differences between samples was determined using
 170 one-way analysis of variance (ANOVA) followed by the post-hoc Tukey's test using Minitab
 171 software. Differences were considered significant at $p < 0.05$.

172 **3. Results and discussion**

173 **3.1 Formation of CHON/CHIT nanocarriers**

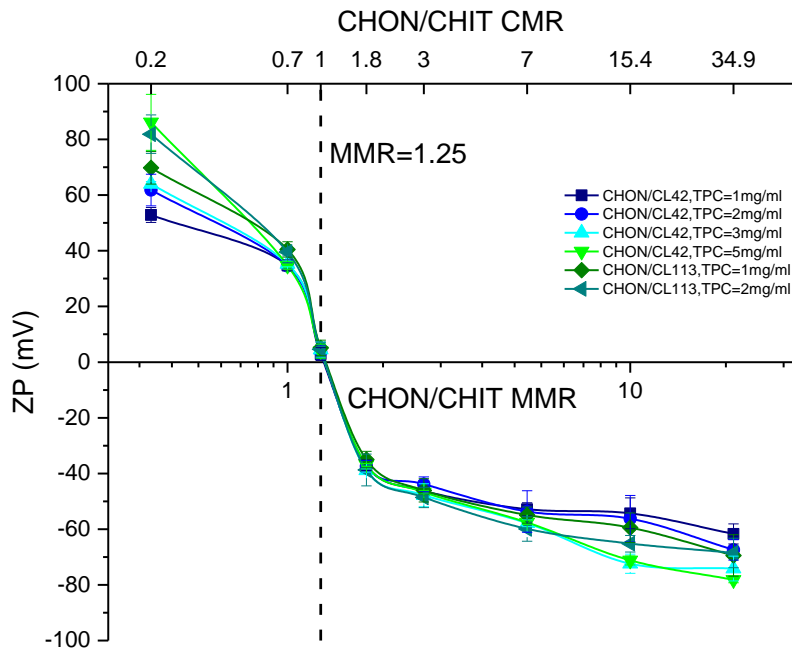
174 The properties of the polymers, particularly the molecular weight, affect the formation
 175 of NPs and their characteristics (Umerska et al., 2012; Polexe and Delair, 2013; Wu and
 176 Delair, 2015). The relevant properties of the polymers are shown in Table 1.

177
 178 Table 1 Physicochemical characteristics of chondroitin sulfate and chitosan salts used in the
 179 studies. DD NMR - degree of deacetylation calculated from nuclear magnetic resonance
 180 data, Mn - number average molecular weight, Mw - weight average molecular weight,
 181 Mw/Mn – dispersity and N/A – not applicable.

Polymer	Counter ion	Counter ion content (% w/w)	DD NMR	Mn (kDa)	Mw (kDa)	Mw/Mn
CHON	Na ⁺	5.55	N/A	33±0.4	59±0.2	1.76±0.011
CL42	Cl ⁻	13.6	84.0%	14±0.1	42±0.9	3.96±0.037
CL113	Cl ⁻	15.5	83.5%	33±7.3	110±6.8	3.38±0.544

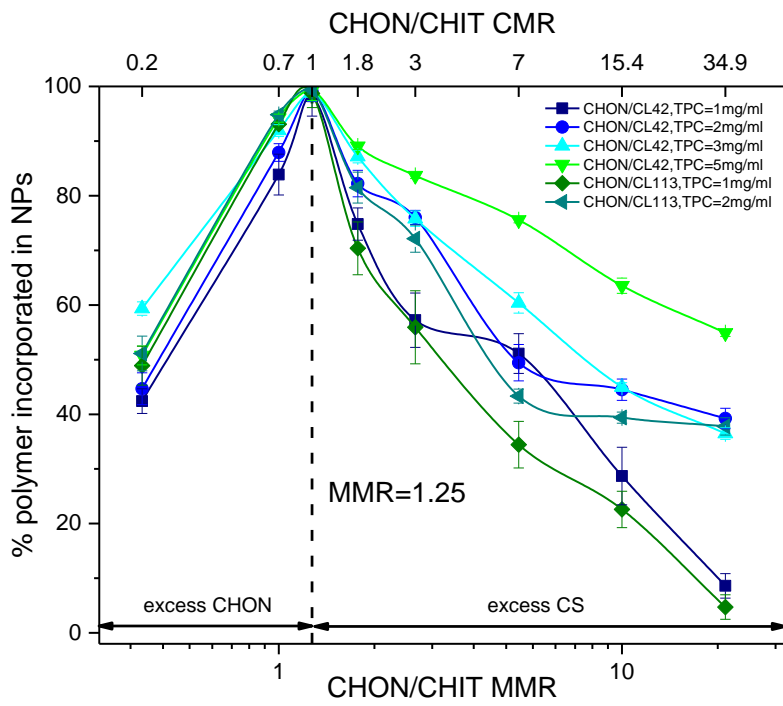
182

183 After mixing the CHON and CHIT solutions it was possible to observe solutions, opalescent
184 or turbid macroscopically homogenous systems or even a phase separation depending on
185 the polymer mixing ratio and concentration. Similar phenomena were observed for other
186 polyelectrolyte complexes, e.g. HA/CHIT (Umerska et al., 2012), HA/PROT (Umerska et al.,
187 2014b), carrageenan/PROT (Dul et al., 2015) and CHON/PROT (Umerska et al., 2015).
188 Interestingly, phase separation for the CHON/CHIT pair was observed only when the
189 CHON/CHIT mass mixing ratio (MMR) was 1.25, regardless of the total polymer
190 concentration (TPC) or the molecular weight of CHIT. The MMR of 1.25 corresponds to a
191 theoretical n^-/n^+ charge mixing ratio (CMR) of 1.20-1.24, where n^- and n^+ are the number of
192 moles of negative and positive charges, respectively. However, the fraction of charged
193 groups on the polyelectrolyte molecules that dissociate depends on pH of medium. The pKa
194 of the amino group of CHIT is approximately 6.5, whereas the pKa of sulfate and carboxyl
195 groups of CHON are 2.6 and 4.6, respectively (Fajardo, Lopes, Valente, Rubira & Muniz,
196 2011). pH of the formulations varied between 4 and 6.5 depending on the mixing ratio and
197 the higher the content of CHIT, the lower the pH of the medium was. In this pH range more
198 than 95% of sulfate groups of CHON should be dissociated, however the dissociation degree
199 varies from 20 to 99% for carboxyl groups of CHON and from 48% to 100% for the amino
200 groups of CHIT. Taking into account the pH and dissociation degree, the actual CMR values
201 that corresponded to MMR=1.25 were between 0.99-1.09, as opposed to 1.20-1.24
202 (theoretical CMR). Indeed, as shown in Figure 1a, the charge inversion occurred close to the
203 CHON/CHIT MMR of 1.25, therefore aggregation at this MMR may be attributed to charge
204 neutralization.



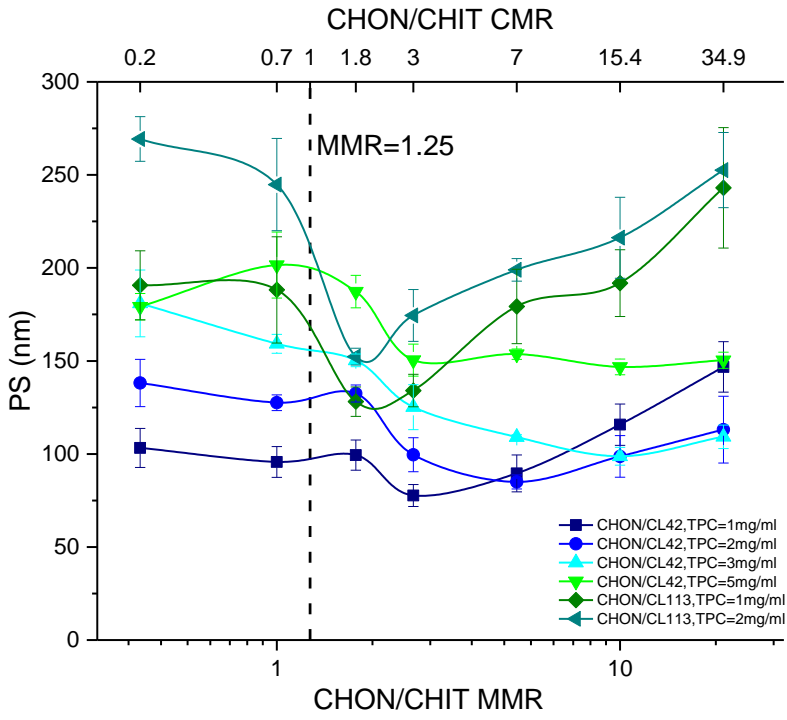
205

a)



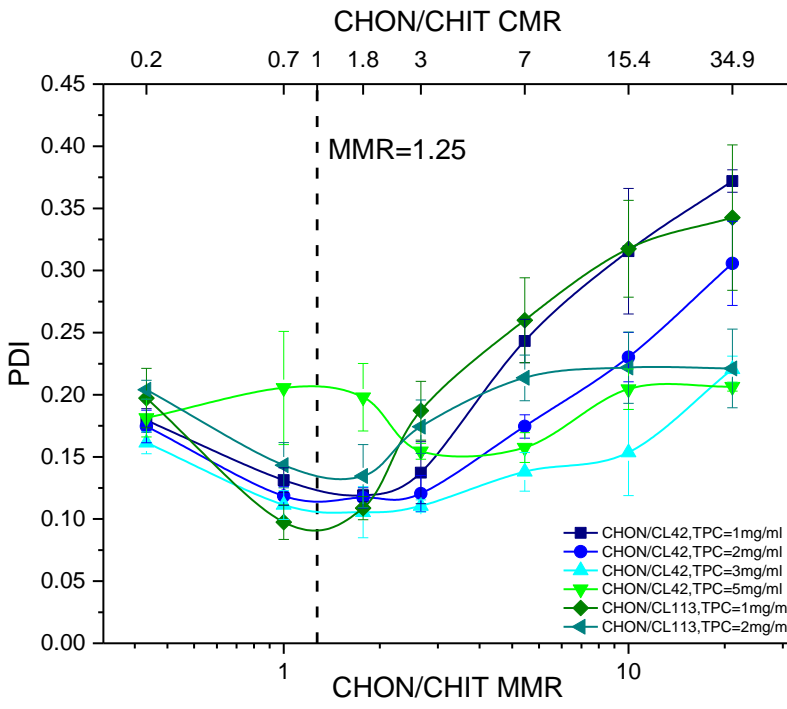
206

b)



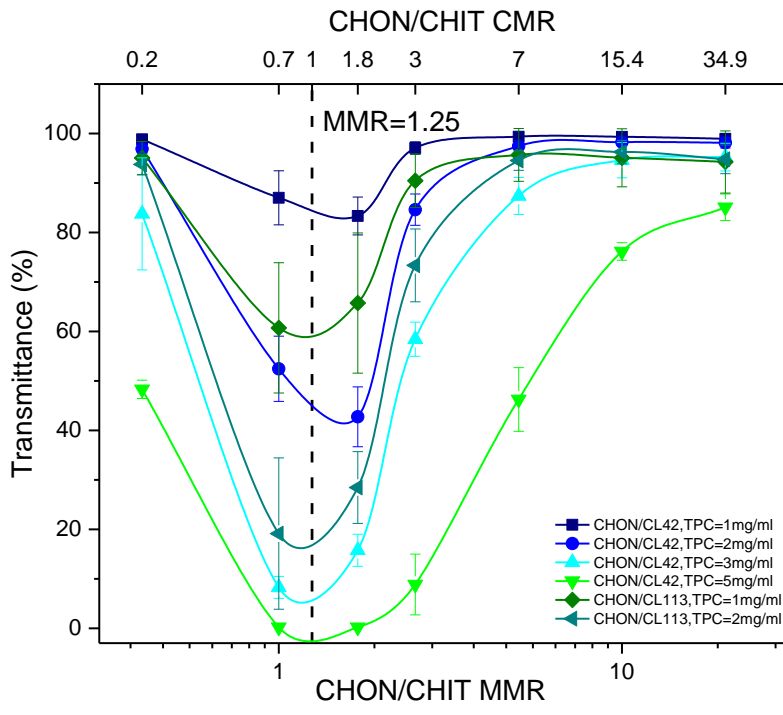
207

c)



208

d)



209

210 Figure 1. Properties of CHON/CHIT NPs: a) zeta potential (ZP), b) percentage of polymer
 211 incorporated into the NPs, c) particle size (PS), d) polydispersity index (PDI) and e)
 212 transmittance (TR). MMR – mass mixing ratio, CMR – charge mixing ratio, TPC – total
 213 polymer concentration.

214

215 The main factor determining the zeta potential was the mixing ratio of the polymers
 216 (Figure 1a). The zeta potential was highly negative for CHON/CHIT MMRs between 1.7 and
 217 20 (CMRs of 1.8-35) and at CHON/CHIT MMRs of 1 and 0.4 (CMRs of 0.7 and 0.2,
 218 respectively) the charge was highly positive. The molecular weight of CHIT appeared to
 219 affect zeta potential of positively charged NPs; CL113-based NPs were characterized by
 220 significantly higher zeta potential values than CL42-NPs at the same CHIT and NP
 221 concentration. The absolute value of zeta potential also increased corresponding to an
 222 increase in TPC, particularly in the case of positively charged NPs. The stability of
 223 polyelectrolyte complex NPs depends on the repulsion between similarly charged NPs and
 224 the net charge must be sufficient if the system is to be physically stable (Umerska et al.,
 225 2015).

226 The amount of polymers incorporated within the NPs is presented in Figure 1b. The
 227 polymer in excess was either CHIT or CHON for positively and negatively charged NPs,

228 respectively. It can be observed, that nearly 100% of the polyelectrolytes were incorporated
229 within the CHON/CHIT MMR=1.25 complexes, therefore this ratio can be considered as
230 stoichiometric. The amount of polymers incorporated within the NPs increased when the
231 MMR was approaching 1.25. The amount of incorporated polymer was also dependent on
232 the TPC- the higher the TPC was, the more polymer was contained within the NPs. The
233 formation of stable polyelectrolyte complex NPs requires that the polyelectrolytes are mixed
234 in non-stoichiometric ratios (Boddohi & Kipper, 2010). Although the dispersions of particles
235 with the MMRs close to 1.25 (i.e. CHON/CHIT MMRs of 1.7 or 1) contain very small amount
236 of free polymer, and for that reason they seem to be more convenient from the quality
237 control point of view, they should be avoided as potential candidates for a drug delivery
238 system, because a small change in pH of the system or addition of a polycationic/polyanionic
239 molecule (for example an active ingredient- a peptide or a nucleic acid) could cause charge
240 neutralization, aggregation and destabilization of the system.

241 Apart from aggregated samples with the CHON/CHIT MMR of 1.25, all tested
242 dispersions were characterized by particles with a small size that varied between 80 and 270
243 nm (Figure 1c). The particle size was influenced by the molecular weight of CHIT, CL113-
244 NPs were larger than CL42-NPs. The particle size was also affected by the TPC. Generally,
245 the higher TPC, the larger was the hydrodynamic diameter of the NPs, however some
246 deviations from this trend were observed. The particle size was also influenced by the
247 CHON/CHIT MMR and the effect exerted by the MMR depended on TPC and molecular
248 weight of CHIT. Generally CHON/CHIT NPs had a homogenous size distribution with PDI
249 values below 0.25 for most of the samples (Figure 1d). Only samples with low TPCs (1
250 mg/ml and in the case of CL42 NPs- also 2 mg/ml) and high CHON/CHIT MMRs (10 for TPC
251 1 mg/ml and 20 for TPC 1 and 2 mg/ml) were characterized by PDI values higher than 0.3.
252 Interestingly, these dispersions contain high percentage of CHON which did not react with
253 CHIT, so the increased PDI values may be due to the contribution of free CHON molecules.

254 Samples with CHON/CHIT MMR=1.25 were not suitable for transmittance
255 measurements. The transmittance of the remaining dispersions is shown in Figure 1e. It can

256 be observed that the turbidity of the samples increased corresponding to an increasing
257 polymer concentration and an increasing molecular weight of CHIT. Another important factor
258 influencing the turbidity of the dispersions was the mixing ratio of the polymers- the turbidity
259 increased when the mass mixing ratio was approaching to 1.25. The transmittance depends
260 on the concentration and the particle size of the complexes. Decreasing value of
261 transmittance corresponding to the CHON/CHIT MMR approaching 1.25 and to an
262 increasing TPC may be an indicator of the formation of larger number of the NPs, particularly
263 for lower TPCs.

264 **3.3 CHON/CHIT/sCT nanoparticles**

265 CHON/CL42 NPs with MMRs of 2.5, 5 and 10 mg/ml at TPCs 1, 2 and 3 mg/ml were
266 selected as potential carriers for sCT (Table 2). Because TPC of 5 mg/ml resulted in the
267 most viscous nano-suspensions with the largest particles, they were not considered as
268 carriers for sCT.

269

270 Table 2 Composition, properties (TR - transmittance, PS - particle size, PDI - polydispersity index and ZP - zeta potential), total n⁻/n⁺ CMR
 271 (charge mixing ratio), percentage of CHON incorporated into the NPs, association efficiency (AE) and drug loading (DL) of sCT-loaded
 272 CHON/CL42 NPs. *p<0.05, **p<0.01, ***p<0.001 versus NPs without sCT.

TPC [mg/ml]	CHON/CL42 mass ratio	Initial conc. sCT (mg/ml)	Total n ⁻ /n ⁺ CMR	CHON incorporated into NPs (%)	AE (%)	DL (%)	TR (%)	PS (nm)	PDI	ZP (mV)
3	2.5	0.5	2.08	80±1**	99.8±0.03	14.26±0.004	19±2***	180±6*	0.214±0.027**	-43.1±1.3
3	5	0.5	3.71	65±1*	99.9±0.02	14.27±0.003	57±3***	220±6**	0.268±0.019**	-59.4±1.4
3	10	0.5	6.12	52±1***	99.8±0.01	14.26±0.001	71±4**	248±11*	0.309±0.038**	-70.0±0.8
3	2.5	1.0	1.84	83±1***	99.5±0.27	24.91±0.068	15±4***	177±13**	0.200±0.016**	-38.5±0.6*
3	5	1.0	3.05	68±1**	99.8±0.04	24.96±0.010	54±2***	211±9*	0.293±0.064*	-52.0±0.9**
3	10	1.0	4.55	55±1***	99.7±0.17	24.94±0.043	72±2**	249±15*	0.356±0.082*	-63.0±1.8*
2	2.5	0.5	1.95	82±1**	99.4±0.23	19.90±0.046	64±4**	140±17*	0.150±0.037	-37.2±2.2*
2	5	0.5	3.34	59±1**	99.7±0.07	19.95±0.014	89±4*	150±34**	0.217±0.060	-52.0±3.4
2	10	0.5	5.21	49±2*	99.8±0.04	19.97±0.008	94±3	162±34*	0.251±0.068	-58.2±8.0
2	2.5	1.0	1.67	83±2**	98.9±0.61	33.09±0.204	34±7***	142±3**	0.182±0.012**	-32.5±1.1**
2	5	1.0	2.61	64±2**	99.6±0.16	33.24±0.053	81±2***	155±2***	0.234±0.017**	-46.0±2.5
2	10	1.0	3.65	49±2*	99.7±0.15	33.27±0.050	90±2**	173±1***	0.306±0.066	-55.1±2.7
1	2.5	0.5	1.67	79±7*	99.3±0.29	33.18±0.097	81±5**	101±13	0.149±0.028	-31.4±2.3**
1	5	0.5	2.61	56±4	99.5±0.08	33.22±0.027	96±1**	95±26	0.215±0.033	-43.8±2.0**
1	10	0.5	3.65	36±2	99.7±0.08	33.27±0.027	98±1	100±22	0.279±0.075	-50.7±4.0

273

274 sCT was very efficiently associated with CHON/CL42 NPs, with the yield close to 100%
275 (Table 2). Moreover, high peptide loading (14-33%) was also achieved. Similar drug loading
276 was accomplished for the previously described HA- and CHON-based nanocarriers
277 (Umerska et al., 2014a; Umerska et al., 2014b; Umerska et al., 2015). The incorporation of
278 an active ingredient can change the properties of the nanocarrier. This is true particularly for
279 the polyelectrolyte complex NPs, which are characterized by a high drug loading. Despite
280 loading of cationic sCT into CHON/CL42 NPs, all tested formulations had strongly negative
281 zeta potential ranging between -31 and -72 mV; in some cases a significant decrease in the
282 absolute value of zeta potential was observed compared with CHON/CHIT NPs with the
283 same TPC and CHON/CHIT MMR (Table 2). The n^-/n^+ CMR calculations confirmed that
284 there is a stoichiometric excess of negative charges in relation to positive charges. The
285 amount of CHON incorporated within CHON/CHIT/sCT NPs was significantly higher than
286 that of CHON/CHIT NPs. Due to its net positive charge the presence of sCT allowed binding
287 of a larger number of CHON molecules within the NPs, decreasing the amount of free
288 polymer. This phenomenon could prevent the charge neutralization and destabilization of the
289 system. For this reason, formulations containing a larger excess of an anionic polymer
290 (CHON in this case) should be preferred for the encapsulation of cationic molecules. This
291 statement can also be true for the opposite situation: in the case of encapsulation of anionic
292 molecules into positively charged NPs the formulation containing higher excess of cationic
293 polymer would be better candidates.

294 All tested CHON/CHIT/sCT NPs had particle diameters varying between 95 and 250
295 nm; in some cases a significant increase was observed compared with CHON/CHIT NPs
296 (Table 2). Inclusion of sCT produced an increase in turbidity of the dispersions, which could
297 be attributed to both, an increase in particle size and in the number of the particles formed.
298 The reduction in negative charge of the NPs and an increase in the turbidity of the system
299 have been observed for different sCT-loaded polyelectrolyte complex NPs, namely
300 CHON/PROT, HA/PROT and HA/CHIT. However the influence of sCT on the particle size
301 varied depending on the type of the carrier. In contrast to CHON/CHIT/sCT, in previously

302 described HA/CHIT NPs either no change or a decrease in particle size was observed for
303 lower and higher sCT concentration, respectively (Umerska et al. 2014a). Only formulation
304 with the lowest MMR tested (2.5) containing high amount of sCT (0.35 mg/ml) showed an
305 increase in particle size. On the other hand, an increase in size was observed for HA/PROT
306 (Umerska et al., 2014b) and in some of the CHON/PROT NPs (Umerska et al., 2015). The
307 increase in particle size in some CHON/CHIT/sCT NPs after incorporation of sCT may be
308 attributed to neutralization of CHON by the polycations (CHIT and sCT) and attainment of
309 more compact structure of the NPs. Indeed, a significant increase in the quantity of CHON
310 incorporated within the NPs was observed in sCT-containing NPs compared with sCT-free
311 NPs.

312 **3.4 CHON/sCT NPs**

313 CHON/sCT complexes obtained by mixing polymer and peptide solutions at different
314 concentrations and different ratios were examined. Similarly to CHON/CHIT system, the
315 mixing of the polysaccharide and peptide solutions yielded different types of systems:
316 solution, an opalescent or turbid dispersion or two-phase systems containing supernatant
317 liquid and aggregates. As shown in Table 3, sCT was bound very efficiently to CHON
318 forming the NPs. Nearly 100% of sCT was complexed to CHON for CHON/sCT MMRs of 0.7
319 and 1.4. Comparable AE was obtained for CHON/sCT MMR of 0.35 at 1 mg/ml of sCT.
320 Therefore, in diluted dispersions such as that containing 0.35 mg/ml CHON, the mass of sCT
321 bound by the polysaccharide was 3 times higher than the mass of CHON. It is probably due
322 to much higher charge density (the number of moles of charges per gram of the compound)
323 in CHON molecules compared with that of sCT molecules.

324

325 Table 3 Composition, properties (TR - transmittance, PS - particle size, PDI - polydispersity index, ZP - zeta potential), total n⁻/n⁺ CMR (charge
 326 mixing ratio), percentage of CHON incorporated into the NPs, association efficiency (AE), and drug loading (DL) of binary CHON/sCT
 327 complexes. MMR – mass mixing ratio.

328

CHON conc. (mg/ml)	sCT conc. (mg/ml)	CHON/sCT MMR	Total n ⁻ /n ⁺ CMR	CHON incorporated into NPs (%)	AE (%)	DL (%)	TR (%)	PS (nm)	PDI	ZP (mV)
0.35	1	0.35	1.41	79±5	94.4±3.96	73.0±3.06	12±2	195±18	0.040±0.013	-15.7±0.5
0.35	2	0.175	0.90	98±3	44.1±14.41	71.6±23.4	0±0	aggregates	N/A	-7.3±0.2
0.7	1	0.7	2.42	76±5	99.7±0.23	58.8±0.14	82±12	99±14	0.227±0.021	-36.8±3.7
0.7	2	0.35	1.41	79±8	95.1±2.39	73.1±1.84	0±0	831±145	0.197±0.034	-14.4±0.2
1.4	1	1.4	4.44	10±8	99.9±0.12	41.6±0.05	99±1	163±13	0.508±0.108	-45.1±0.7
1.4	2	0.7	2.42	66±5	99.8±0.16	58.8±0.10	51±10	120±20	0.135±0.016	-38.4±1.8

329

330 Additionally, CHON molecules only have anionic moieties, whereas sCT, bearing net
331 positive charge at neutral and acidic pH, apart from cationic amino acids also contains
332 anionic amino acids. When the CHON/sCT MMR was further decreased to 0.175, phase
333 separation occurred immediately after mixing the sCT and CHON solutions and 56% of sCT
334 was found in the non-associated fraction. Hence, at CHON/sCT MMR of at least 0.35,
335 CHON was able to efficiently bind sCT, but with a further decrease in CHON/sCT MMR the
336 binding places in CHON molecules became saturated and sCT molecules not involved in the
337 interactions with CHON were separated from the CHON/sCT complex by ultrafiltration-
338 centrifugation. CHON/sCT dispersions had an excellent loading capacity and stable
339 CHON/sCT NPs contained up to 73% (w/w) of sCT.

340 The zeta potential of CHON/sCT complexes was markedly affected by the
341 CHON/sCT MMR (Table 3). All tested dispersions contained negatively charged particles,
342 however in the case of CHON/sCT MMR of 0.175 dispersion, where the aggregation was
343 observed, the value of zeta potential was only -7 mV, indicating neutralization of the anionic
344 groups of CHON by sCT. The negative surface charge can be attributed to the dominant
345 presence of CHON molecules on the particle surface. The quantity of CHON bound within
346 the nanoplexes was dependent on the CHON/sCT MMR; the lower the MMR was, the higher
347 amount of CHON was present in the nanoplexes.

348 The turbidity of the dispersions increased correspondingly to a decrease in
349 CHON/sCT MMR (Table 3). Apart from the dispersion with the CHON/sCT MMR of 0.175,
350 other tested dispersions contained the particles with sizes in the nano range. Similarly to the
351 previously described HA/sCT complexes (Umerska et al., 2014a), the excess of the anionic
352 polysaccharide increased the solubility of its complexes with sCT. Apart from the CHON/sCT
353 MMR of 1.4 dispersion, which was not suitable for DLS analysis as it did not meet quality
354 criteria, all other dispersions were homogeneously dispersed with PDI values below 0.25. It is
355 possible that in the CHON/sCT MMR of 1.4 dispersion the excess of CHON was responsible
356 for the increase in the solubility of the CHON/sCT complex and the decrease in the amount
357 of particles. As the amount of sCT was relatively low compared with CHON, the competition

358 between CHON molecules for binding with cationic groups of sCT may have resulted in the
359 formation of highly disordered NPs with relatively low density.

360 In summary, after mixing CHON and sCT solutions at CHON/sCT MMRs of 0.35 and
361 0.7 it was possible to obtain stable nanoparticulate dispersions (Table 3). This phenomenon
362 was not observed for HA/sCT complexes described previously (Umerska et al., 2014a).
363 Although an HA/sCT complex was formed, as demonstrated by transmittance, viscosity
364 measurements and by FTIR, only two types of systems were formed: soluble complexes and
365 unstable NPs (having the appearance of a solution) or two-phase systems. Phase
366 separation was observed at HA/sCT MMRs of 0.44 and 0.33. Interestingly, hyaluronic
367 acid/sCT MMR of 0.33 corresponds to total n^-/n^+ CMR of 0.72, whereas CHON/sCT MMR of
368 0.35- to total n^-/n^+ CMR of 1.41; the former yielded phase separation, whereas the latter-
369 stable NPs. Difference in the CMRs is due to the presence of two ionizable groups in each
370 disaccharide unit of CHON molecules in contrast to HA, where only one carboxylic group is
371 present in each disaccharide unit. Although the CMR influences the appearance of the
372 system, particularly the phase separation due to charge neutralization which occurs at CMR
373 values close to 1, it does not explain the formation of stable NPs for the CHON/sCT system
374 and not for the HA/sCT system, as in the case of HA/sCT system the formation of stable
375 NPs was not observed for the CMR between 0.33 and 2.83. HA contains only weak acid
376 carboxylic groups in its molecules whereas CHON contains both weak and strong acid
377 carboxylic and sulfate groups, respectively (Denuziere et al., 1996). For this reason the
378 former can be considered as a weak polyelectrolyte, whereas the latter- as a strong
379 polyelectrolyte. Both, the higher charge density of CHON and the higher strength of CHON
380 complexes compared with HA may cause the formation of more compact structures yielding
381 stable CHON/sCT NPs. The smaller molecular weight of CHON (50 kDa) compared with that
382 of HA (257 kDa) may also contribute to the better colloidal stability of the former complexes
383 with sCT.

384 **3.5 Colloidal behavior of CHON/sCT and CHON/CL42/sCT NPs in various media**

385 Apart from the particle characteristics the properties of polyelectrolyte complex NPs
 386 also depend on the properties of the dispersant, such as ionic strength and pH (Umerska et
 387 al., 2012, Umerska et al., 2015). Three formulations (Table 4) were selected for stability
 388 studies: two CHON/CL42/sCT NP formulations with CHON/CL42 MMRs of 5 and 2.5 and
 389 sCT of 1 mg/ml and one CHON/sCT formulation (CHON=1.4 mg/ml, sCT=2 mg/ml).

390 Table 4. Properties of CHON/CL42/sCT and CHON/sCT NPs in different media. The
 391 samples were prepared as described in Sections 2.3 and 2.5.2 and measured after 1 hour or
 392 24 hours of incubation at 37° C. TPC – total polymer concentration, MMR – mass mixing
 393 ratio, PS - particle size, PDI - polydispersity index, ZP - zeta potential, (D) – diluted. *p<0.05,
 394 **p<0.01, ***p<0.001 versus NPs in water, #p<0.05, ##p<0.01, ###p<0.001 versus NPs stored
 395 for 1 hour.

TPC of 3 mg/ml, CHON/CL42 MMR of 2.5, sCT of 1 mg/ml NPs						
Medium	1h PS (nm)	24h PS (nm)	1h PDI	24h PDI	1h ZP (mV)	24h ZP (mV)
Water	182±13	179±13	0.180±0.029	0.174±0.022	-37.6±1.3	-34.5±6.4
Acetate buffer (D)	190±25	192±23	0.160±0.044	0.143±0.032	-25.1±2.7**	-27.1±4.9
Acetate buffer	228±2**	252±2###	0.101±0.028*	0.097±0.025	-26.4±0.6***	-26.2±0.7
PBS (D)	175±1	179±1##	0.130±0.035	0.159±0.031	-31.4±1.1**	-28.8±0.4#
PBS	aggregation		aggregation		aggregation	
HCl	683±114**	648±147	0.192±0.079	0.149±0.110	4.1±5.6***	5.0±6.3
TPC of 2 mg/ml, CHON/CL42 MMR of 5, sCT of 1 mg/ml NPs						
Medium	1h PS (nm)	24h PS (nm)	1h PDI	24h PDI	1h ZP (mV)	24h ZP (mV)
Water	168±14	175±3	0.250±0.008	0.259±0.004	-48.1±7.2	-47.2±3.4
Acetate buffer (D)	188±5	188±5	0.265±0.008	0.262±0.006	-32.1±1.8*	-32.6±0.6
Acetate buffer	206±9*	224±6#	0.175±0.007***	0.167±0.015	-26.8±0.1**	-28.8±1.8
PBS (D)	162±6	163±8	0.238±0.005	0.240±0.007	-32.0±6.6*	-26.0±9.7
PBS	351±2***	663±13###	0.155±0.011***	0.256±0.010###	-25.9±2.7**	-23.8±0.6
HCl	400±113*	435±116	0.144±0.023**	0.149±0.022	-2.5±2.1***	-3.6±0.9
CHON/sCT NPs (CHON of 1.4 mg/ml, sCT of 2.0 mg/ml)						
Medium	1h PS (nm)	24h PS (nm)	1h PDI	24h PDI	1h ZP (mV)	24h ZP (mV)
Water	120±20	126±9	0.139±0.031	0.160±0.029	-39.8±2.0	-38.5±2.8
Acetate buffer (D)	134±7	152±3#	0.096±0.011	0.080±0.031	-27.0±0.1***	-27.2±0.6
Acetate buffer	283±55**	467±42##	0.120±0.012	0.230±0.014###	-25.0±2.0***	-23.3±2.9
PBS (D)	232±39*	276±28	0.328±0.062**	0.455±0.119	-16.2±0.7***	-15.2±6.2
PBS	282±21***	251±34	0.533±0.088**	0.602±0.128	-8.8±1.3***	-5.1±2.5
HCl	761±202**	1120±103#	0.376±0.097*	0.531±0.073#	-12.5±0.1***	-12.6±0.6

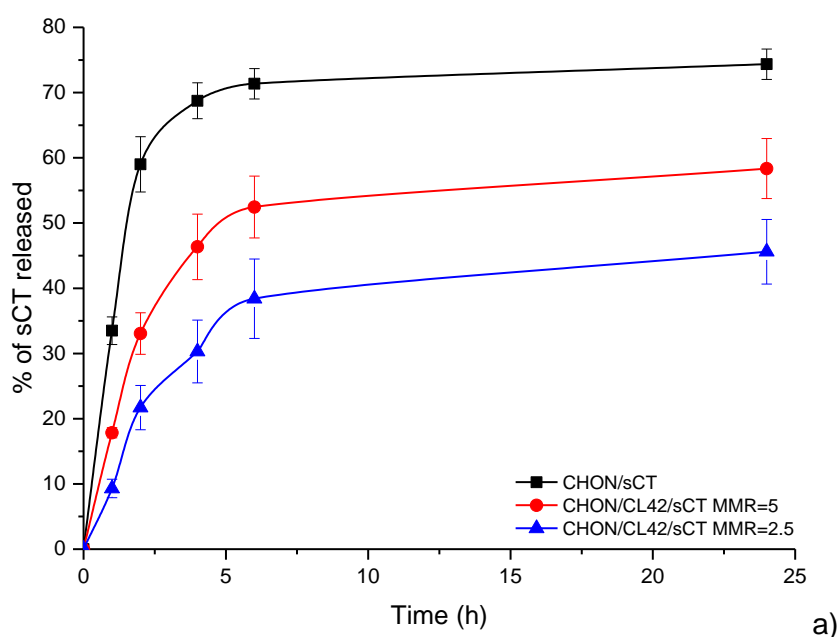
396 It can be observed that the particle size of all tested formulations increased in PBS, acetate
397 buffer and in HCl (Table 4). In the case of CHON/CL42 MMR=2.5 formulation an immediate
398 formation of aggregates was observed in PBS. The increase in particle size can be attributed
399 an increased ionic strength of the medium. Indeed, in diluted acetate buffer or diluted PBS
400 no significant change was observed except CHON/sCT NPs, which significantly increased
401 their size in diluted PBS. A significant decrease in PDI was observed in acetate buffer for
402 both CHON/CL42/sCT formulations; moreover, in the case of formulation with CHON/CL42
403 MMR of 5 a significant decrease was also observed in PBS and HCl. In contrast to
404 CHON/CL42/sCT formulations, CHON/sCT formulations became significantly more
405 polydispersed in diluted PBS, PBS and HCl. The absolute value of zeta potential was
406 significantly reduced in all tested media for all tested formulations. The reduction of surface
407 charge was especially pronounced in HCl for CHON/CL42/sCT formulations; for NPs with a
408 CHON/CL42 MMR=2.5 the inversion from negative to positive zeta potential was observed.
409 This may be attributed to a decrease in ionization of CHON at such low pH values. Similarly
410 to CHON/PROT NPs described previously (Umerska et al., 2015), the chloride anion
411 appeared to exert a stronger effect on the properties of the CHON/CHIT/sCT and
412 CHON/sCT NPs than the acetate.

413 Two different effects govern the behavior of polyelectrolyte complexes after a
414 subsequent change in the ionic strength of the medium, namely secondary aggregation or
415 dissolution, depending on the nature of the components of the system (Dautzenberg, 2000).
416 It has been shown that CHON-based NPs retain sodium chloride from PBS or HCl (in the
417 case of HCl this salt can be formed from the sodium ion originating from CHON) or sodium
418 acetate from the acetate buffer. The salts present in the polymer network can decrease
419 ionization and therefore the charge density of polymer molecules. The secondary
420 aggregation may occur in the case of CHON/CHIT/sCT NPs. The reduction in charge density
421 of polyelectrolytes will induce a decrease in the macromolecules stiffness, as a result of the
422 decreased repulsive electrostatic interactions. Therefore, conformational adaptation required
423 for the charge matching should be easier, thus leading to more compact complexes (Wu &

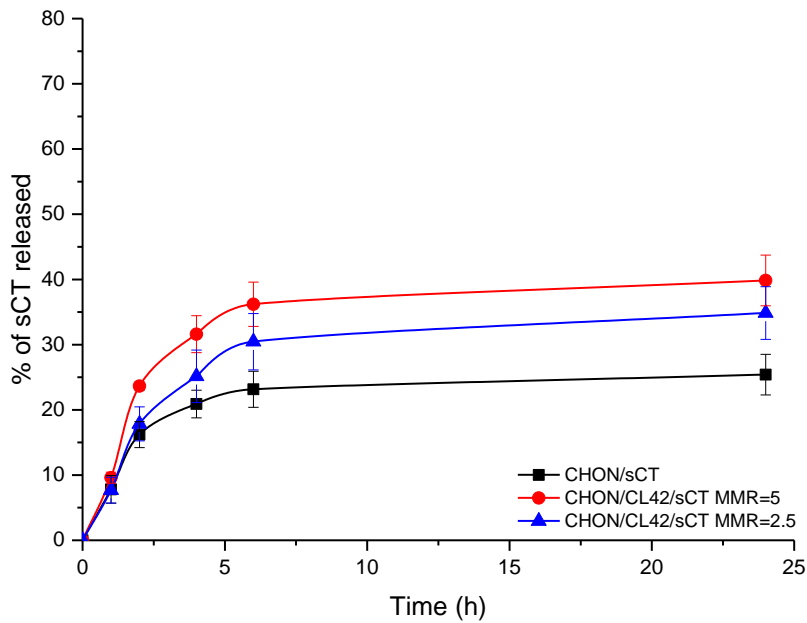
424 Delair, 2015). A decrease in PDI in CHON/CHIT/sCT NPs could be an indication of the
425 formation of more ordered and compact nanostructures, whereas the increased particle size
426 suggests the incorporation of a larger quantity of polyelectrolyte molecules per nanoparticle.
427 The increase in ionic strength and rearrangement between the polyelectrolyte molecules
428 also leads to release of sCT molecules (see Section 3.6). For CHON/sCT systems, it is likely
429 than in PBS or in HCl dissolution of the complexes occurs. The release of sCT molecules
430 should lead to dissociation of the binary complex, as CHON cannot self-assemble into NPs
431 in an aqueous medium (Zhao et al., 2015). Although an increase in the particle size was
432 observed, high PDI values (0.46-0.6) indicate that these results are not reliable. A change in
433 pH and an increase in ionic strength leads at first to weakening the bonds between CHON
434 and sCT (a fraction of disordered, large particles with low density) and then to dissociation of
435 the complex. Because DLS is more sensitive to larger particles, the obtained result reflects
436 their presence.

437 3.6 *In vitro* release of sCT

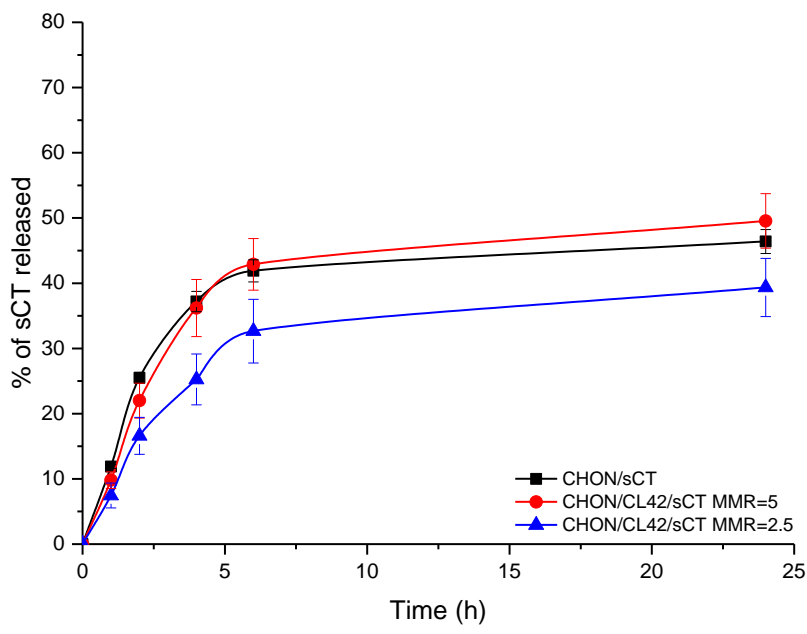
438 Figure 2 shows the cumulative release of sCT from CHON/CL42/sCT and
439 CHON/sCT NPs.



440



441



442

443 Figure 2 Cumulative release of sCT from CHON/sCT NPs (CHON of 1.4 mg/ml, sCT of 2.0
 444 mg/ml - black squares), TPC of 2 mg/ml, CHON/CL42 MMR of 5, sCT of 1 mg/ml NPs (red
 445 circles) and TPC of 3 mg/ml, CHON/CL42 MMR of 2.5, sCT of 1 mg/ml NPs (blue triangles)
 446 into (a) PBS, (b) acetate buffer and (c) HCl solution. MMR – mass mixing ratio.

447

448 The release of sCT from its nanocomplex with CHON was influenced by the dispersant and
 449 the composition of the nanocarrier. Similarly to the previously described CHON/PROT/sCT
 450 NPs (Umerska et al., 2015), almost no sCT was released either to water or to diluted acetate
 451 buffer from all tested formulations.

452 CHON/CHIT/sCT NPs with MMR=2.5 released similar % of sCT into PBS, acetate
453 buffer and HCl after 24 hours ($46\pm5\%$, $35\pm4\%$ and $40\pm4\%$, respectively, Figure 2). Similar
454 behavior was observed for CHON/CHIT/sCT NPs MMR=5, which released $58\pm5\%$, $40\pm4\%$
455 and $50\pm4\%$ after 24 hours into PBS, acetate buffer and HCl, respectively. Release of sCT
456 from CHON/sCT NPs was influenced by the release medium to a larger extent than that of
457 CHON/CHIT/sCT NPs. The amount of sCT released from CHON/sCT complexes after 24
458 hours into PBS, acetate buffer and HCl was $74\pm2\%$, $25\pm3\%$ and $46\pm2\%$, respectively.
459 Interestingly, the size of these NPs in HCl was $\sim 600\%$ of the initial size in water compared to
460 only $\sim 200\%$ in PBS and acetate buffer. Time- and pH-dependent release of CHON from
461 CHON/CHIT complexes was observed by Fajardo et al. (2011) with the greatest release of
462 CHON occurring at pH around neutral (pH=6 and pH=8) and lowest at pH=2. Dissociation
463 and detachment of the principal polymer (CHON) constituting the NPs should lead to
464 breaking up the complex with sCT (and/or CHIT) that occurs in PBS but not in HCl and thus
465 resulting in the greater release of the peptide in PBS. As discussed in Section 3.5, the
466 observed increase in the particle size seen in HCl may be caused by incorporation a quantity
467 of chloride as sodium chloride (the sodium ion originating from CHON used as a sodium
468 salt). However, as the PDI values of these formulations are quite high (0.38-0.60), the
469 particle size measurements are not as reliable as at low PDI values (below 0.25) and should
470 be interpreted with caution.

471 The most significant differences in sCT release were observed for PBS. The release
472 rate decreased in the following order: CHON/sCT NPs > CHON/CHIT/sCT NPs MMR=5 >
473 CHON/CHIT/sCT NPs MMR=2.5, as reflected by decreasing values of the rate constant k
474 (Table 5).

475
476 Table 5 Model parameter estimates and related goodness of fit statistics for sCT release
477 from CHON/sCT NPs (CHON of 1.4 mg/ml, sCT of 2.0 mg/ml), TPC of 2 mg/ml, CHON/CL42
478 MMR of 5, sCT of 1 mg/ml NPs TPC of 3 mg/ml, CHON/CHIT MMR of 2.5, sCT of 1 mg/ml
479 NPs data fitted to the first order model, where W_{∞} is the amount of sCT released at infinity
480 and k is the release rate constant.

Medium	k (h ⁻¹)	W _∞ (μg/mg of NPs)	Goodness of fit (R ²)
CHON/sCT NPs (CHON of 1.4 mg/ml, sCT of 2.0 mg/ml)			
Acetate buffer	0.446±0.021	149±16	0.989
HCl	0.371±0.003	276±11	0.993
PBS	0.689±0.045	434±13	0.992
CHON/CHIT/sCT NPs TPC of 2 mg/ml, CHON/CL42 MMR of 5, sCT of 1 mg/ml			
Acetate buffer	0.387±0.040	134±15	0.984
HCl	0.294±0.003	168±15	0.994
PBS	0.397±0.007	194±16	0.998
CHON/CHIT/sCT NPs TPC of 3 mg/ml, CHON/CHIT MMR of 2.5, sCT of 1 mg/ml			
Acetate buffer	0.320±0.025	88±10	0.991
HCl	0.259±0.022	100±11	0.997
PBS	0.285±0.023	114±13	0.992

481

482 This study confirms that release of peptide from ionic hydrogels depend on the
483 composition of the complex and on the environmental conditions. The fact that the quantity
484 of sCT released into acetate buffer was smaller than that released into HCl or PBS may be
485 due to the fact that at pH 5 electrostatic interactions between sCT and CHON are optimal
486 due to maximal ionization of both molecules. At acidic pH ionization of anionic groups of
487 CHON is considerably decreased, whereas at pH 7.4 the degree of ionization of sCT could
488 be smaller- the histidine group (pKa 6.10) should be dissociated at pH=5, but not at pH=7.4.
489 The higher release from CHON/sCT NPs compared with that from CHON/CHIT/sCT NPs
490 could be attributed to the lower density of the former NPs. The dense network of CHON and
491 CHIT chains may retard the diffusion of sCT.

492 Based on the results of release studies and stability in different buffers it can be
493 concluded that NPs containing large quantities of CHIT are not good candidates for
494 intravenous administration due to the possibility of aggregation. On the other hand, the
495 CHON/CHIT/sCT NPs, particularly those with CHON/CHIT MMR=2.5 are capable of
496 providing a prolonged sCT release and for that reason they could be good candidates for
497 other forms of parenterals, e.g. for intramuscular administration. The advantage of

498 CHON/CHIT/sCT NPs is the mucoadhesive properties of CHIT and for this reason they
499 could make interesting candidates for oral delivery. Furthermore, the CHON/CHIT/sCT NPs
500 showed better stability in HCl than CHON/sCT NPs. The aggregation process of the CHIT-
501 containing NPs in PBS could be a major disadvantage, however before approaching the
502 intestines the NPs would be diluted and that could prevent possible aggregation. The
503 CHON/sCT NPs would be good candidates as they do not aggregate and the complex
504 dissolves in PBS. Moreover, when administration in a final solid state formulation is
505 necessary, the CHON/sCT NPs with high drug loading are preferred due to dilution issues
506 (excipient addition) associated with forming such dosage forms.

507 **4. Summary and conclusions**

508 Both, positively and negatively charged CHON/CHIT NPs have been successfully
509 developed and characterized. The formation and the physicochemical properties of
510 CHON/CHIT NPs were depended on polymer mixing ratio, polymer concentration and
511 molecular weight of CHIT. NPs containing polymers at the ratio far from stoichiometric would
512 make better carriers for ionized drugs as they are less susceptible to charge neutralization
513 and physical destabilization. sCT was successfully loaded into CHON/CHIT NPs with
514 efficiency close to 100% and notably high sCT loading (up to 33%).

515 A new type of NPs composed of CHON and sCT (a binary system) has been
516 successfully developed and characterized. Some of these carriers offer the advantage of a
517 very high drug loading up to 73% and high association efficiency (95%).

518 The particle size of all tested formulations increased in PBS, acetate buffer and in
519 HCl compared to that in water, however most of them remained in the nano-range even after
520 24 hours. Both, the media and the composition of the nanocarriers were found to affect the
521 release of sCT. In all tested formulations the % of sCT released and the quantity of sCT
522 released per mg of NPs at infinity decreased in the following order: PBS>HCl>acetate buffer.
523 CHON/sCT NPs released the largest % of sCT, whereas CHON/CHIT/sCT MMR=2.5 NPs
524 released the smallest quantity of sCT.

525 **Acknowledgements**

526 This study was supported by the Irish Drug Delivery Research Network, a Strategic
527 Research Cluster grant (07/SRC/B1154) under the National Development Plan co-funded by
528 EU Structural Funds and Science Foundation Ireland and the Synthesis and Solid State
529 Pharmaceutical Centre funded by Science Foundation Ireland under grant number
530 12/RC/2275.

531 **Conflict of interest**

532 The authors declare that there are no conflicts of interest.

533 **References**

534 Baldrick, P. (2010). The safety of chitosan as a pharmaceutical excipient. *Regulatory*
535 *Toxicology and Pharmacology*, 56, 290-299.

536 Benhabiles, M.S., Salah, R., Lounici, H., Drouiche, N., Goosen, M. F. A., & Mameri,
537 N. (2012). Antibacterial activity of chitin, chitosan and its oligomers prepared from shrimp
538 shell waste. *Food Hydrocolloids*, 29, 48-56.

539 Boddohi, S., & Kipper, M. J., 2010. Engineering nanoassemblies of polysaccharides.
540 *Advanced Materials*, 22, 2998-3016.

541 Dautzenberg, H. (2000). Light scattering studies on polyelectrolyte complexes.
542 *Macromolecular Symposia*, 162, 1-21

543 Denuziere, A., Ferrier, D., & Domard, A. (1996). Chitosan- chondroitin sulfate and
544 chitosan-hyaluronate polyelectrolyte complexes. Physico-chemical aspects. *Carbohydrate*
545 *Polymers*, 29, 317-323.

546 Dul, M., Paluch, K. J., Kelly, H., Healy, A. M., Sasse, A., & Tajber, L. (2015). Self-
547 assembled carrageenan/protamine polyelectrolyte nanoplexes- Investigation of critical
548 parameters governing their formation and characteristics. *Carbohydrate Polymers*, 123, 339-
549 349.

550 Fajardo, A. R., Lopes, L. C., Valente, A. J. M., Rubira, A. F., & Muniz, E. C. (2011).
551 Effect of stoichiometry and pH on the structure and properties of Chitosan/Chondroitin
552 sulfate complexes. *Colloid and Polymer Science*, 289, 1739-1748.

553 Fröhlich, E. (2012). The role of surface charge in cellular uptake and cytotoxicity of
554 medical nanoparticles. *International Journal of Nanomedicine*, 7, 5577-5591.

555 Goole, J., Lindley, D. J., Roth, W., Carl, S. M., Amighi, K., Kauffmann, J. M., & Knipp,
556 G. T. (2012). The effects of excipients on transporter mediated absorption. *International*
557 *Journal of Pharmaceutics*, 393, 17-31.

558 Hagiwara, K., Nakata, M., Koyama, Y., & Sato, T. (2012). The effects of coating
559 pDNA/chitosan complexes with chondroitin sulfate on physicochemical characteristics and
560 cell transfection. *Biomaterials*, 33, 7251-7260.

561 Hou, Y., Hu, J., Park, H., & Lee, M. (2012). Chitosan-based nanoparticles as a
562 sustained protein release carrier for tissue engineering applications. *Journal of Biomedical*
563 *Materials Research A*, 100A, 939-947.

564 Hu, C.-S., Tang, S.-L., Chaing, C.-H., Hosseinkhani, H., Hong, P.-D., & Yeh, M.-K.
565 (2014). Characterization and anti-tumor effects of chondroitin sulfate-chitosan nanoparticles
566 delivery system. *Journal of Nanoparticle Research*, 16, 2672

567 Paluch, K. J., Tajber, L., McCabe, T., O'Brien, J. E., Corrigan, O. I., & Healy, A. M.
568 (2010). Preparation and solid state characterisation of chlorothiazide sodium intermolecular
569 self-assembly suprastructure. *European Journal of Pharmaceutical Sciences*, 41, 603-611.

570 Parojčić, J., Stojković, A., Tajber, L., Grbić, S., Paluch, K. J., Djurić, Z., & Corrigan,
571 O. I. (2011). Biopharmaceutical characterization of ciprofloxacin HCl-ferrous sulfate
572 interaction. *Journal of Pharmaceutical Sciences*, 100, 5174-5184.

573 Place, L. W., Sekyi, M., & Kipper, M. J. (2014). Aggrecan-Mimetic,
574 Glycosaminoglycan-Containing Nanoparticles for Growth Factor Stabilization and Delivery.
575 *Biomacromolecules*, 15, 680-689.

576 Polexe, R. C., & Delair, T. (2013). Elaboration of stable and antibody functionalized
577 positively charged colloids by polyelectrolyte complexation between chitosan and hyaluronic
578 acid. *Molecules*, 18, 8563-8578.

579 Pusateri, A. E., McCarthy, S. J., Gregory, K. W., Harris, R. A., Cardenas, L.,
580 McManus, A. T., & Goodwin, C.W. (2003). Effect of a Chitosan-Based Hemostatic Dressing

581 on Blood Loss and Survival in a Model of Severe Venous Hemorrhage and Hepatic Injury in
582 Swine. *The Journal of Trauma: Injury, Infection, and Critical Care*, 54, 177-182.

583 Ryan, S. M., McMorrow, J., Umerska, A., Patel, H. B., Kornerup, K. N., Tajber, L.,
584 Murphy, E. P., Perretti, M., Corrigan, O. I., & Brayden, D. (2013). An intra-articular salmon-
585 calcitonin based nanocomplex reduces experimental inflammatory arthritis. *Journal of*
586 *Controlled Release*, 167, 120-129.

587 Santo, V. E., Gomes, M. E., Mano, J. F., & Reis, R. L. (2012). Chitosan-chondroitin
588 sulfate nanoparticles for controlled delivery of platelet lysates in bone regenerative medicine.
589 *Journal of Tissue Engineering and Regenerative Medicine*, 6, s47-s59.

590 Sogias, I. A., Williams, A. C., & Khutoryanskiy, V. V. (2008). Why is chitosan
591 mucoadhesive? *Biomacromolecules*, 9, 1837-1842.

592 Tsai, H.-Y., Chiu, C.-C., Lin, P.-C., Chen, S.-H., Huang, S.-J., & Wang, L.-F. (2011).
593 Antitumor Efficacy of Doxorubicin Released from Crosslinked Nanoparticulate Chondroitin
594 Sulfate/Chitosan Polyelectrolyte Complexes. *Macromolecular Bioscience*, 11, 680-688.

595 Umerska, A., Paluch, K. J., Inkielewicz-Stepniak, I., Santos-Martinez, M. J., Corrigan,
596 O. I., Medina, C., & Tajber, L. (2012). Exploring the assembly process and properties of
597 novel crosslinker-free hyaluronate-based polyelectrolyte colpmex nanoparticles. *International*
598 *Journal of Pharmaceutics*, 436, 75-87.

599 Umerska, A., Corrigan, O. I., & Tajber, L. (2014a). Intermolecular interactions
600 between salmon calcitonin, hyaluronate, and chitosan and their impact on the process of
601 formation and properties of peptide-loaded nanoparticles. *International Journal of*
602 *Pharmaceutics*, 477, 102-112.

603 Umerska, A., Paluch, K. J., Santos-Martinez, M.-J., Corrigan, O. I., Medina, C., &
604 Tajber, L. (2014b). Self-assembled hyaluronate/protamine polyelectrolyte nanoplexes:
605 synthesis, stability, biocompatibility and potential use as peptide carriers. *Journal of*
606 *Biomedical Nanotechnology*, 10, 3658-3673.

607 Umerska, A., Paluch, K. J., Santos-Martinez, M. J., Medina, C., Corrigan, O. I., &
608 Tajber, L. (2015). Chondroitin-based nanoplexes as peptide delivery systems –Investigations

609 into the self-assembly process, solid-state and extended release characteristics. *European*
610 *Journal of Pharmaceutics and Biopharmaceutics*, 93, 242-253.

611 van Damme, M.-P. I., Moss, J. M., Murphy, W. H., & Preston, B. N. (1994). Binding
612 properties of glycosaminoglycans to lysozyme- effect of salt and molecular weight. *Archives*
613 *of Biochemistry and Biophysics*, 310, 16-24.

614 Volpi, N. (2002). Oral bioavailability of chondroitin sulfate (Condrosulf®) and its
615 constituents in healthy men volunteers. *Osteoarthritis and Cartilage*, 10, 768-777.

616 Wu, D., & Delair, T. (2015). Stabilization of chitosan/hyaluronan colloidal
617 polyelectrolyte complexes in physiological conditions. *Carbohydrate Polymers*, 119, 149-
618 158.

619 Yeh, M.-K., Cheng, K.-M., Hu, C.-S., Huang, Y.-C., & Young, J.-J. (2011). Novel
620 protein-loaded chondroitin sulfate-chitosan nanoparticles: Preparation and characterization.
621 *Acta Biomaterialia*, 7, 3804-3812.

622 Zhao, L., Liu, M., Wang, J., & Zhai, G. (2015). Chondroitin sulfate-based nanocarriers
623 for drug/gene delivery. *Carbohydrate Polymers*, 133, 391-399.